Reviews

EPR spectroscopy of thermally induced and light-induced spin transitions in heterospin exchange clusters of compounds $Cu(hfac)_2L^R$*

M. V. Fedin,[a] S. L. Veber,[a,b] R. Z. Sagdeev,[a] V. I. Ovcharenko,[a] and E. G. Bagryanskaya[a]*

[a]*International Tomography Center, Siberian Branch of the Russian Academy of Sciences, 3a ul. Institutskaya, 630090 Novosibirsk, Russian Federation. Fax: +7 (383) 333 1399. E-mail: mfedin@tomo.nsc.ru*
[b]*Novosibirsk State University, 2 ul. Pirogova, 630090 Novosibirsk, Russian Federation.*

The review summarizes the results of EPR investigations of magneto-structural anomalies occurring in exchange-coupled copper-nitroxide clusters belonging to the family of compounds $Cu(hfac)_2L^R$. The key features and potential of EPR spectroscopy in studies of such systems, the methods developed to determine the exchange constants, and experiments using the optical switching of magnetic parameters in the heterospin exchange clusters studied are discussed.

Key words: spin transitions, EPR spectroscopy, heterospin exchange clusters, exchange interaction.

Introduction

Exchange-coupled complexes of transition-metal ions with stable nitroxide radicals (NR) play an important role in the research on molecular magnetism and have been intensively studied in the recent decades.[1—23] In addition to the static magnetic susceptibility technique and X-ray diffraction analysis, in many cases EPR spectroscopy becomes a key method of investigations of the structural and magnetic properties of such exchange-coupled systems.[24—31] This review is devoted to a new class of molecular magnetics, *viz.*, "breathing crystals" and summarizes for the first time the results of systematic EPR investigations of thermally induced and light-induced spin transitions in these compounds.[32—38]

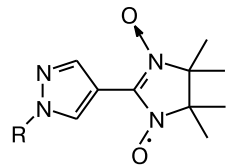

L^R

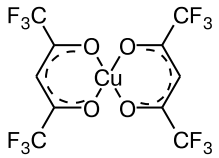

$Cu(hfac)_2$

R = Me, Et, Pr^n, Bu^n

The family of heterospin "breathing crystals" $Cu(hfac)_2L^R$ based on copper(II) hexafluoroacetylacetonate and pyrazolyl-substituted nitronyl-nitroxides was discovered quite recently.[39—43] The solid phases of these compounds have polymer-chain structures with two different ("head-to-

* Dedicated to Academician of the Russian Academy of Sciences I. L. Eremenko on the occasion of his 60th birthday.

Published in Russian in *Izvestiya Akademii Nauk. Seriya Khimicheskaya,* No. 6, pp. 1043—1058, June, 2010.
1066-5285/10/5906-1065

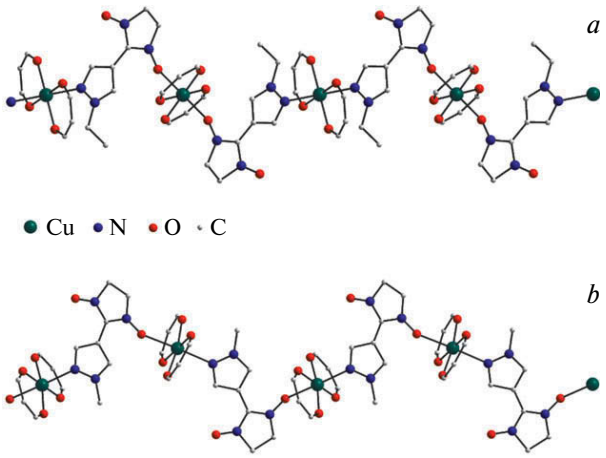

Fig. 1. Polymeric chains with the "head-to-head" motif in the structure of $Cu(hfac)_2L^{Et}$ (*a*) and with the "head-to-tail" motif in the structure of $Cu(hfac)_2L^{Me}$ (*b*).*

head" and "head-to-tail") motifs of coordination of the nitroxide radical and Cu^{2+} ion (Fig. 1). The "head-to-head" coordination leads to formation of a chain comprising alternating one- and three-spin fragments >N—Cu^{2+}—N< and >N—O•—Cu^{2+}—•O—N<, respectively. The "head-to-tail" coordination results in a regular polymer chain comprising two-spin fragments >N—O•—Cu^{2+}—N<. It was found that the compounds in question exhibit reversible thermally induced structural rearrangements accompanied by anomalies in the magnetic behavior and that in some cases the $\mu_{eff}(T)$ or $\chi T(T)$ dependences are similar in character to the classical spin crossover. Of course, spin crossover cannot occur in Cu^{2+} because of its electronic configuration (d^9), but for a heterospin complex of Cu^{2+} with a nitroxide radical there is a possibility of changing the electronic configuration of the whole cluster. For instance, in most compounds under consideration, the Cu^{2+}—O bonds in the fragments >N—O•—Cu^{2+}—•O—N< are significantly shortened (up to 0.3 Å) on lowering the temperature; this leads to an increase in antiferromagnetic exchange coupling and to effective pairing of two out of three spins in the spin triad. As a result, the magnetic moment decreases (Fig. 2). A fundamental difference between the classical spin crossover and its nonclassical version in "breathing crystals" is that in the former case one deals with the change in the electronic configuration of

* Figures 1 and 6 are available in full color in the on-line version of the journal (http://www.springerlink.com).

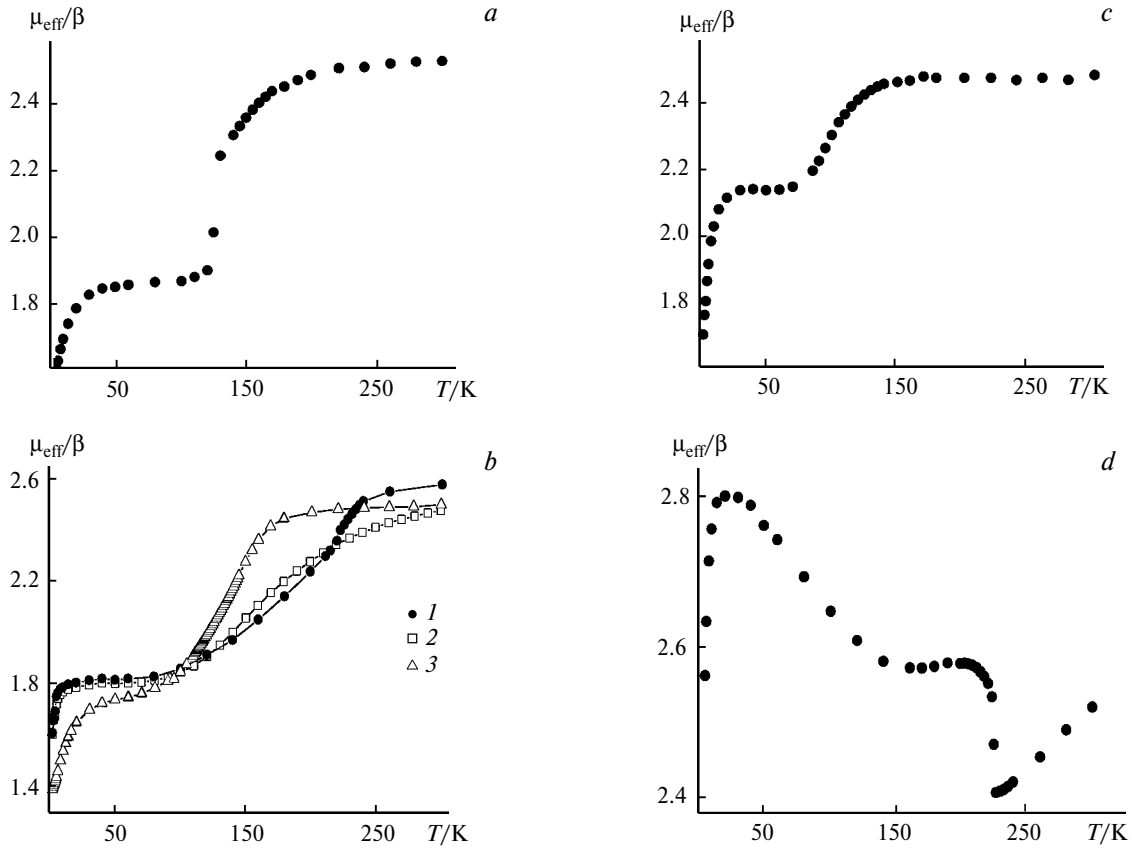

Fig. 2. Temperature dependences of the effective magnetic moment of "breathing crystals": $Cu(hfac)_2L^{Bu^n}\cdot 0.5C_7H_{16}$ (*a*); $Cu(hfac)_2L^{Pr^n}$(*b*, curve *1*), $Cu(hfac)_2L^{Bu^n}\cdot 0.5C_8H_{10}$ (*b*, curve *2*), and $Cu(hfac)_2L^{Bu^n}\cdot 0.5C_7H_{16}$ (*b*, curve *3*); $Cu(hfac)_2L^{Bu^n}\cdot 0.5C_8H_{18}$ (*c*); and $Cu(hfac)_2L^{Et}$ (*d*).

the d-shell of single paramagnetic centers (metal ions), whereas the latter case involves changes in the electronic interaction and configuration in the environment of the metal ion. In this respect, nonclassical spin transitions (crossover) in "breathing crystals" can be much more sensitive to external factors, which in turn offers new prospects for efficient manipulation of their magnetic properties. For instance, it was found that the characteristic parameters of spin transitions in "breathing crystals" strongly depend on the substituent (R) in the pyrazolyl fragment of the nitroxide radical (R = Me, Et, Pr^n, Bu^n), and on the organic solvent, which can be incorporated into the interchain space in the crystal, because in both cases the packing parameters of the polymeric chains are changed (see Fig. 2). In this connection, "breathing crystals" are of paramount interest for both basic research and, in the future, for the design of novel functional materials with unusual magnetic properties.

All magnetic anomalies observed in the "breathing crystals" are related to structural rearrangements in the coordination sites including two- and three-spin systems. The theory of EPR of two- and three-spin exchange-coupled clusters has been well developed because such systems are used as models in studies of more complex exchange clusters. Comprehensive reviews of theoretical and experimental research were reported in monographs.[24,44] When the exchange interaction characterized by the exchange interaction constant J is weak or comparable in magnitude with the external magnetic field ($|J| << B$ or $|J| \approx B$, respectively), the EPR spectra exhibit splitting of spectral lines of individual paramagnetic centers and/or additional transitions whose positions depend on the magnitude of the exchange constant. If the exchange interaction is much stronger than the external magnetic field ($|J| >> B$), the EPR spectra of two-spin systems correspond to only a triplet state with the effective average g-factor $g = (g_1 + g_2)/2$, where g_1 and g_2 are the individual g-factors of the exchange-coupled spins. In principle, the temperature dependence of the intensity of this spectral line characterizes the relative populations of the triplet and singlet terms and allows one to estimate the exchange constant and to determine its sign. However, in most cases the accuracy of this method is low. For three-spin systems, one should expect the appearance of three EPR lines corresponding to three terms of the system (a quartet term and two doublet terms) if their populations are comparable with one another, or a single line otherwise. Experimental EPR spectra of three-spin clusters based on Cu^{2+} trinuclear complexes and on Cu^{2+} complexes with stable radicals exhibit a single EPR line with an average value of the g-factor.[45—49] A slight temperature dependence of the position of this line was explained as being due to mixing of different terms and by temperature dependences of the populations of different terms. However, because of the ratio of J and thermal energy (kT), the temperature-induced shift of the resonance line and the typical changes in the EPR spectra were insignificant and precluded quantitative studies of exchange interactions. Thus, EPR spectroscopy is usually inappropriate for the determination of the constants of the exchange interactions in the cluster if the exchange interaction is strong ($|J| >> B$).

We have found that the EPR spectra of "breathing crystals" $Cu(hfac)_2L^R$ exhibit a number of specific features, which permits successful characterization of spin transitions and the exchange interaction in their heterospin exchange clusters.[32—38] For these systems, the exchange interaction constants J become comparable with the thermal energy (kT) at $T \approx 20$—300 K. Moreover, owing to structural rearrangements, the exchange interaction constants become temperature-dependent. As a result, the EPR spectra significantly change upon temperature variation. Detailed analysis of all spectra corresponding to these changes allows one to study the temperature dependences of exchange interaction constants and the dynamics of spin states. Here we report on the key features of EPR spectroscopy of strongly coupled spin triads of "breathing crystals" and the methods developed to study the spin transitions and exchange interactions in these systems. In addition, we will dwell on the optical manipulation of the magnetic properties of "breathing crystals" and, in some cases, the possibility of measuring the constants of the intercluster exchange interaction.

EPR spectroscopy of exchange-coupled spin triads of "breathing crystals": key features

In the vast majority of "breathing crystals" $Cu(hfac)_2L^R$ synthesized to date, the polymeric chains have the "head-to-head" motif. In this case, the polymer structure is built of alternating coordination sites CuN_2O_4 and CuO_6 containing, respectively, one-spin systems >N—Cu^{2+}—N< and three-spin clusters >N—•O—Cu^{2+}—O•—N< coupled by a strong exchange interaction ($J \approx 10$—100 cm^{-1}, see Fig. 1, *a*). Although structural rearrangements lead to changes in the geometric parameters of both types of clusters, the observed magnetic anomalies are to a greater extent due to changes in the magnetic parameters of the three-spin cluster (triad).

The spin Hamiltonian of a symmetric spin triad can be written as follows:

$$\hat{H} = \beta \boldsymbol{B} \boldsymbol{g}^{R}(\boldsymbol{S}^{R^1} + \boldsymbol{S}^{R^2}) + \beta \boldsymbol{B} \boldsymbol{g}^{Cu} \boldsymbol{S}^{Cu} - 2J(\boldsymbol{S}^{R^1} + \boldsymbol{S}^{R^2})\boldsymbol{S}^{Cu} - 2J' \boldsymbol{S}^{R^1} \boldsymbol{S}^{R^2}, \quad (1)$$

where the superscripts R^1, R^2, and Cu refer to the nitroxide radicals R^1 and R^2 and to the copper ion, respectively; $\boldsymbol{S}^R$ and $\boldsymbol{S}^{Cu}$ are the spins of the radical and the copper ion, respectively; $\boldsymbol{g}^R$ and $\boldsymbol{g}^{Cu}$ are the g-tensors of the radical and the copper ion, respectively (it is assumed that nitroxide radicals are magnetically equivalent and are charac-

terized by isotropic g-tensors ($\boldsymbol{g}^{R}$), *i.e*, $\boldsymbol{g}^{R} = g^{R}\hat{\mathbf{1}}$, where $\hat{\mathbf{1}}$ is the unit matrix), the magnetic field $\boldsymbol{B} = [0,0,B]$ is parallel to the Z axis; J is the constant of the exchange interaction between the copper ion and each radical, and J' is the constant of the exchange interaction between the radicals ($J < 0$ corresponds to antiferromagnetic interaction). Usually, for a linear spin triad one has $J' << J$ and therefore the last term in Eq. (1) can be neglected in all cases considered in the present work.

The energy levels of the spin triad are shown in Fig. 3. The spin multiplets of the triad (two doublet states and one quartet state) are described by individual g-tensors $\boldsymbol{g}^{A}$, $\boldsymbol{g}^{B}$, and $\boldsymbol{g}^{C}$ (see Refs 24 and 47):

$$\begin{aligned} \boldsymbol{g}^{A} &= (4g^{R}\hat{\mathbf{1}} - \boldsymbol{g}^{Cu})/3, \\ \boldsymbol{g}^{B} &= \boldsymbol{g}^{Cu}, \\ \boldsymbol{g}^{C} &= (2g^{R}\hat{\mathbf{1}} + \boldsymbol{g}^{Cu})/3. \end{aligned} \qquad (2)$$

The allowed transitions in the EPR spectra include the $|1\rangle \leftrightarrow |2\rangle$, $|2\rangle \leftrightarrow |3\rangle$ and $|3\rangle \leftrightarrow |4\rangle$ transitions between the levels of the quartet state C, the $|5\rangle \leftrightarrow |6\rangle$ transition between the levels of the doublet B, and the $|7\rangle \leftrightarrow |8\rangle$ transition between the levels of the doublet A (see Fig. 3).

We found that unusual EPR spectra of these three-spin systems coupled by strong exchange interaction are due to predominant population of the ground spin state at relatively high temperatures (typically, ~100—200 K) and mixing (spin exchange) of different multiplets of the spin system.

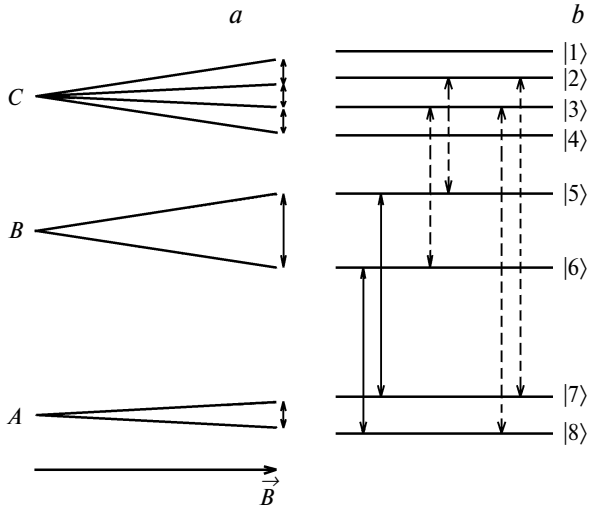

Fig. 3. A scheme of energy levels for a spin triad in the magnetic field $\boldsymbol{B}$. Arrows denote the allowed EPR transitions within the multiplets A, B, and C (*a*). Energy level diagram for the spin triad and transitions. Solid arrows denote the transitions induced by modulation of the isotropic and anisotropic exchange interactions and dashed arrows denote the transitions induced by modulation of the anisotropic exchange interaction only (*b*).

Typical temperature dependences of EPR spectra are shown in Fig. 4 taking the spectra of $Cu(hfac)_2L^{Pr^n}$ as examples. Despite the fact that all individual constituents of the three-spin cluster (Cu^{2+} and the nitroxide radical) are characterized by $g > 2$, the low-temperature EPR spectra exhibit intense signals in the region $g < 2$. This can be explained by predominant population of the ground spin state of the cluster (doublet A) with the effective g-factor $g < 2$ (see expression (2)). Such a 'polarization' of spin multiplets appears at temperatures $kT < |J|$ (for $J \approx 100$ cm^{-1}, one has $T < 140$ K); the populations of the upper doublet B and quartet C are low and their EPR signals are not observed. It should be noted that the results of quantum chemical calculations of the g-factors of "breathing crystals" are in good agreement with experimental data and also suggest the presence of signals with $g < 2$ at low temperatures.[50]

Experimental studies of the temperature dependences of the Q- and W-band EPR spectra (35 and 94 GHz, respectively) of these compounds revealed yet another important effect. One would expect that temperature variations will affect only the relative intensities of the lines of the multiplets A, B, and C in proportion to the changes in their Boltzmann populations. However, in most cases a single EPR line of the three-spin cluster instead of three groups of lines with $\boldsymbol{g}^{A}$, $\boldsymbol{g}^{B}$, and $\boldsymbol{g}^{C}$ is experimentally observed in the whole temperature range from $kT << |J|$ to $kT >> |J|$; the position of this line is temperature-dependent (Fig. 5). This temperature behavior can be explained by some effects similar to the so-called spin (or frequency) exchange between different EPR lines.

Each spin triad can be found in the state A, B or C with the corresponding probabilities specified by the Boltzmann distribution. The effective g-factors of the multiplets A, B,

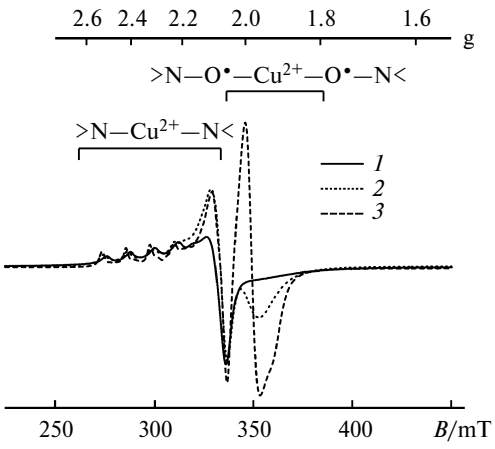

Fig. 4. X-band (9 GHz) EPR spectra of polycrystalline $Cu(hfac)_2L^{Pr^n}$ at 260 (*1*), 140 (*2*), and 90 K (*3*). A schematic assignment of EPR signals to magnetically isolated copper ions in the fragments >N—Cu^{2+}—N< and spin triads in the fragments >N—O•—Cu^{2+}—•O—N< is shown.

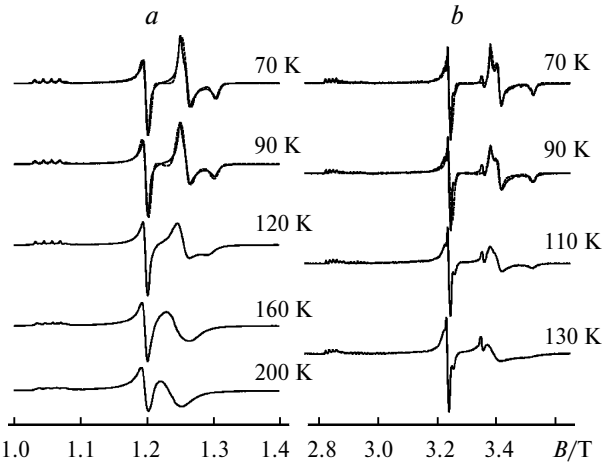

Fig. 5. Temperature dependences of EPR spectra of polycrystalline $Cu(hfac)_2L^{Pr^n}$ at 34 (*a*) and 94 GHz (*b*). The results of theoretical simulation are shown by dashed lines.

and *C* are different and, therefore, the EPR transitions within each multiplet are characterized by different frequencies. Assume that each triad continuously undergoes stochastic transitions between different multiplet states. In other words, the spin jumps randomly from one environment within the triad (one multiplet) to another. As a result, the Larmor frequency of the electron spin randomly varies between the corresponding frequencies of the multiplets *A*, *B*, and *C*. The process is similar to fast changes in the molecular geometry leading to changes in the magnetic parameters (*e.g.*, *g*-factor or the chemical shift). In this respect, the spin exchange between different spectral lines is well known in EPR and NMR spectra. In our case, fast transitions between different multiplets of the spin triad can be considered as spin "jumps" from one multiplet to another. If the rate of such "jumps" is high compared to the Larmor frequency difference between different multiplets (fast exchange), a single EPR line at the "center of gravity" of the spectrum will be observed experimentally. Temperature variations will change the contributions of the EPR lines of different multiplets; as a result, the "center of gravity" of the spectrum and, therefore, the averaged EPR line, will be shifted, as is observed experimentally. We have shown[33] that taking account of the dynamic spin exchange in simulation of EPR spectra allows the temperature dependence of the position of the line of the spin triad to be reproduced qualitatively; quantitative analysis requires knowledge of the temperature dependence of the exchange constant $J(T)$.

It seems logical to asume that the dynamic spin exchange is due to phonon-assisted modulation of the exchange interaction between the spins of Cu^{2+} and nitroxide radical. Since structural rearrangements are accompanied by changes in the Cu—O distances, these bonds are nonrigid. This makes a large-amplitude modulation of Cu—O distances quite probable, which leads to modulation of the exchange interaction, which is strongly dependent on the distance between paramagnetic centers. Modulation of isotropic exchange interaction causes transitions between the doublets *A* and *B* while transitions to the quartet state *C* are forbidden. However, taking account of the modulation of anisotropic exchange interaction removes this forbiddenness and leads to efficient mixing of all multiplets (*A*, *B*, and *C*). Our estimates[33] showed that the rates of transitions between the multiplets *A* and *B* in the spin triads of "breathing crystals" can be as high as 10^{12} s^{-1} (10^8—10^{10} s^{-1} for the transitions involving the multiplet *C*). The high rates of transitions are due to rather strong exchange coupling (of the order of 100 cm^{-1}) because strong exchange interaction leads to a high modulation field. In addition, the high rates of transitions between the multiplets can be due to the fact that the transition frequencies are much closer to the maximum of the phonon density distribution than, *e.g.*, the frequencies of EPR transitions between the Zeeman levels.

However, on the one hand, the exchange interactions in most "breathing crystals" significantly weaken at high temperatures as a result of a phase spin transition (to $J \approx 1$—10 cm^{-1}) and, thus, modulation of exchange interaction by local vibrations of the crystal lattice no longer explains the observed high mixing rates. On the other hand, at high temperatures, it is natural to expect manifestaton of the dynamic Jahn—Teller effect in copper ions; this can lead to much higher rates of spin exchange. Most probably, the observed spin exchange effects are due to both these interrelated processes and further theoretical and experimental studies can make it possible to separate and interpret their contributions.

Depending on the frequency of the EPR spectrometer, dynamic spin exchange can be fast, intermediate, or slow; experiments in different frequency ranges allow one to study its rates. We studied the rates of spin exchange (dynamic mixing) of three "breathing crystals" in a wide range of EPR frequencies from 34 to 244 GHz.[38] Indeed, the Q-band EPR spectra of three complexes ($Cu(hfac)_2L^{Pr^n}$, $Cu(hfac)_2L^{Bu^n} \cdot 0.5C_8H_{10}$, and $Cu(hfac)_2L^{Bu^n} \cdot 0.5C_8H_{18}$) correspond to fast exchange (one averaged EPR line of the spin triad) (Fig. 6). At the same time, the spectra of $Cu(hfac)_2L^{Pr^n}$ and $Cu(hfac)_2L^{Bu^n} \cdot 0.5C_8H_{10}$ recorded at 122 and 244 GHz exhibit a resolved structure of the lines of the spin triad, *viz.*, two lines (with $g < 2$ and $g > 2$) whose intensities gradually redistribute in the temperature range from about 100 to 200 K (Fig. 6, *b*). Thus, at 244 GHz one deals with a slow spin exchange in $Cu(hfac)_2L^{Pr^n}$ and $Cu(hfac)_2L^{Bu^n} \cdot 0.5C_8H_{10}$. The EPR spectra of $Cu(hfac)_2L^{Bu^n} \cdot 0.5C_8H_{18}$ recorded in all frequency ranges (34, 122, and 244 GHz) and in the temperature range 50—300 K show a single averaged line of the spin triad, which corresponds to fast spin exchange (see Figs 6, *c* and 6, *d*). Analysis of the temperature depen-

dence of the width of this line showed that at 244 GHz the limit of infinitely fast exchange is not reached and the linewidth has a well-defined maximum at about 110 K. At the same time, in the Q-band the linewidth monotonically increases with temperature and it may be inferred that the limit of infinitely fast exchange is reached.

Spin exchange (dynamic mixing) in the triads of "breathing crystals" was described using the formalism of the modified Bloch equations.[33,51] Approximation of the EPR spectra by simulation in three frequency ranges (34, 122, and 244 GHz) simultaneously for each temperature made it possible to determine the mixing rates; depending on temperature, they are in the range 10^9—10^{12} s^{-1} and higher.

Manifestation of spin transitions: a theoretical description

At temperatures $kT \approx |J|$ and $kT > |J|$, assuming that the condition for fast spin exchange between different multiplets is met (this is typical at microwave frequencies $\nu_{mw} < 94$ GHz), the position and shape of the averaged EPR line of the spin triad show a temperature-dependent behavior. In the case of fast spin exchange, the effective g-tensor of the spin triad corresponds to the "center of gravity" of the spectrum and can be written as follows:

$$\boldsymbol{g}_{\text{eff}}(T) = \sum_{I=A,B,C} \boldsymbol{g}^I P_B^I \Big/ \sum_{I=A,B,C} P_B^I = \frac{\boldsymbol{g}^A P_B^A + \boldsymbol{g}^B P_B^B + \boldsymbol{g}^C P_B^C}{P_B^A + P_B^B + P_B^C} \qquad (3)$$

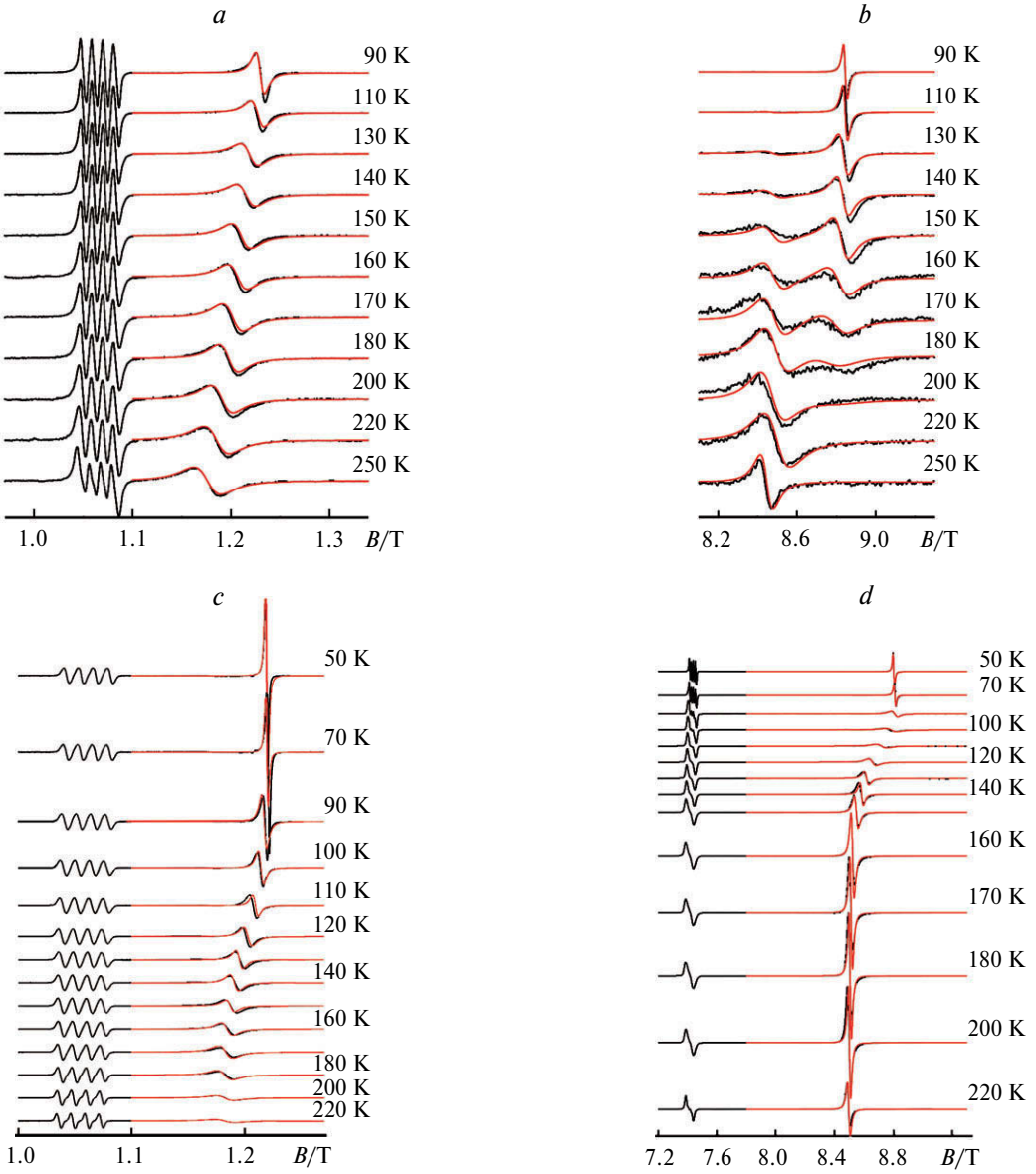

Fig. 6. Temperature dependences of EPR spectra of single crystals of $Cu(hfac)_2L^{Pr^n}$ (*a*, *b*) and $Cu(hfac)_2L^{Bu^n} \cdot 0.5C_8H_{18}$ (*c*, *d*) at 34 (*a*, *c*) and 244 GHz (*b*, *d*). The results of theoretical simulation are shown in red.

where the coefficients P^{I}_{B} characterize the probability of absorption of microwave energy by an electron in the states *A*, *B*, or *C*, respectively. The coefficients P^{I}_{B} include the Boltzmann populations of the levels, the number of EPR transitions for each multiplet, and the corresponding probabilities of EPR transitions

$$P^{I}_{B} = e^{-E^{I}/kT} \sum_{i} p_{i}^{I} \quad (4)$$

where p_i^I are the intensities of the EPR transitions within the multiplet *I*. One EPR transition is allowed between the levels of the multiplet *A* ($|7\rangle \leftrightarrow |8\rangle$), one EPR transition is allowed between the levels of the multiplet *B* ($|5\rangle \leftrightarrow |6\rangle$), and three transitions are allowed between the levels of the multiplet *C* ($|1\rangle \leftrightarrow |2\rangle$, $|2\rangle \leftrightarrow |3\rangle$ and $|3\rangle \leftrightarrow |4\rangle$). The intensities of the corresponding transitions are proportional to the matrix elements

$$m^2_{ij} = |\langle i|\hat{S}_x|j\rangle|^2$$

which are as follows: $m_{12}{}^2 = m_{34}{}^2 = 3$, $m_{23}{}^2 = 4$ and $m_{56}{}^2 = m_{78}{}^2 = 1$. Using these expressions and Eqs (2)—(4), one gets

$$\boldsymbol{g}_{\text{eff}}(T) = \frac{\boldsymbol{g}^{A} + \boldsymbol{g}^{B} \cdot e^{2J/kT} + 10\boldsymbol{g}^{C} \cdot e^{3J/kT}}{1 + e^{2J/kT} + 10e^{3J/kT}} =$$
$$= \frac{(4\boldsymbol{g}^{R} - \boldsymbol{g}^{Cu}) + 3\boldsymbol{g}^{Cu} \cdot e^{2J/kT} + 10(2\boldsymbol{g}^{R} + \boldsymbol{g}^{Cu}) \cdot e^{3J/kT}}{3(1 + e^{2J/kT} + 10e^{3J/kT})}. \quad (5)$$

In the high-temperature limit $|J|/kT \approx 0$, one gets $\boldsymbol{g}_{\text{eff}} = \boldsymbol{g}^{C}$ because, according to expression (2), one has $\boldsymbol{g}^{A} + \boldsymbol{g}^{B} = 2\boldsymbol{g}^{C}$. In the low-temperature limit $|J|/kT >> 1$ ($J < 0$), one gets $\boldsymbol{g}_{\text{eff}} = \boldsymbol{g}^{A}$. This means that for typical average (isotropic) values $g^A = 1.96$ and $g^C = 2.05$ the effective *g*-factor should change by about $\Delta\boldsymbol{g}_{\text{eff}} \approx 0.1$ upon temperature variation. At 94 GHz (W-band), this corresponds to a shift of the resonance magnetic field by about 150 mT. This value is rather large and the shift can easily be observed experimentally. The effective *g*-factor can vary smoothly or in a sterwise manner, depending on which function $J(T)$ is used. It should be noted that the ratio $g_{\text{eff}} \approx g^R \approx 2$ is achieved at $|J| \approx kT$ ($J < 0$); this can be shown with ease using Eqs (5) and (2). Therefore, the temperature at which the line of the spin triad reaches the value $g = 2$ can be used for a simple estimation of the exchange constant at this temperature. Another useful observation is that at $|J|/kT \approx 2$ ($J < 0$) the effective *g*-factor (g_{eff}) almost reaches a minimum value g^A: the extent of transformation $g_{\text{eff}} = g^C \rightarrow g_{\text{eff}} = g^A$ is about 90%, which can also be used for evaluation of the parameter *J*. These two methods of estimation of the exchange constant using the dependence of g_{eff} on the parameter $|J|/kT$ calculated from Eq. (5) for typical values of the average (isotropic) *g*-factors $g^A = 1.96$, $g^B = 2.15$, and $g^C = 2.05$ are illustrated in Fig. 7, which also shows the temperature dependence of the magnetic moment of the spin triad calculated from the equation

$$\mu^2_{\text{eff}} = \frac{3(g^{A})^2 + 3(g^{B})^2 \cdot e^{2J/kT} + 30(g^{C})^2 \cdot e^{3J/kT}}{8(1 + e^{2J/kT} + 2e^{3J/kT})} +$$
$$+ 0.5\mu_{\text{is,eff}}{}^2, \quad (6)$$

which can be derived with ease by analogy with the expression for the effective *g*-factor ($\mu_{\text{is,eff}} \approx 1.86$ is the magnetic moment of a one-spin system). As can be seen, the curves of the effective magnetic moment and the effective *g*-factor are somewhat different in shape; this indicates a difference in information extracted from them.

Diversity of spin transitions and their manifestation in EPR

The theoretical model developed provides a correct explanation for the transformation of EPR spectra with temperature and allows the exchange interaction constant to be estimated. We studied compounds $Cu(hfac)_2L^R$ with different substituents R (R = Me, Et, Pr^n, and Bu^n) and different organic solvents (Solv) present in the crystal structures ($Cu(hfac)_2L^R \cdot 0.5Solv$). Here we present a number of examples illustrating different types of spin transitions in "breathing crystals", their manifestations in EPR spectra, and an analysis using the approach developed.

Compound $Cu(hfac)_2L^{Bu^n} \cdot 0.5C_7H_{16}$ undergoes an abrupt spin transition at $T_c \approx 125$ K, which causes the effective magnetic moment to decrease by $\Delta\mu_{\text{eff}} \approx 0.35$ within the temperature range $\Delta T_c \approx 10$ K (see Fig. 2, *a*). The overall decrease in the magnetic moment between $T = 300$ and $T = 50$ K is $\Delta\mu_{\text{eff}} \approx 2.53—1.85 = 0.68$. The magnetic behavior at temperatures below ~25 K is governed by intercluster exchange interactions between different paramagnetic centers of the polymeric chains. Using Fig. 7, one can establish a simple correlation between the manifestation of spin transitions in the mag-

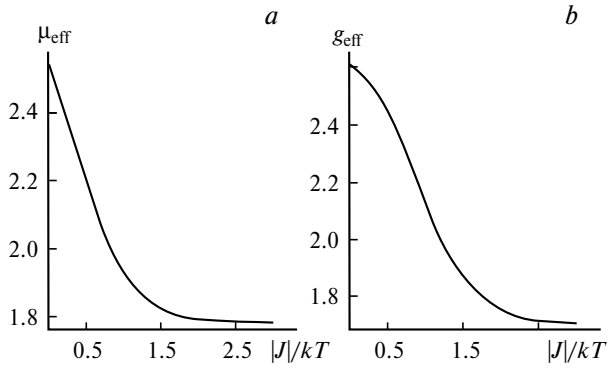

Fig. 7. Theoretical dependences of the effective magnetic moment (*a*) and effective *g*-factor (*b*) of the spin triad on the parameter $|J|/kT$ calculated using Eqs (5) and (6), respectively.

netic susceptibility and EPR measurements for $Cu(hfac)_2L^{Bu^n} \cdot 0.5C_7H_{16}$. On the one hand, a decrease in the magnetic moment by $\Delta\mu_{eff} \approx 0.7$ to $\mu_{eff} \approx 1.85$ corresponds to the transition of the system from the state $|J|/kT \ll 1$ to the state $|J|/kT > 1$ (see. Fig. 7, *a*). On the other hand, at $|J|/kT > 1$ one should expect $g_{eff} < 2$ and, therefore, intense EPR signals should be observed in a high field (see Fig. 7, *b*). Of course, Eq. (6) and Fig. 7 are only suitable for approximate evaluation because consideration of exact *g*-factors and intercluster exchange interactions will affect the absolute values of $\mu_{eff}(|J|/kT)$. Thus, EPR spectroscopy data provide 'more direct' information on exchange interaction in the spin triad because this allows one to exactly determine the *g*-factors; in addition, the contributions of the one- and three-spin clusters are spectrally separated. The EPR spectra of $Cu(hfac)_2L^{Bu^n} \cdot 0.5C_7H_{16}$ exhibit significant changes near the transition temperature; as a result, very intense signals with $g < 2$ at $T < 130$ K are detected; these signals are well-resolved even in the X-band (Fig. 8). This pattern of the EPR spectra unambiguously indicates that the condition $|J|/kT > 1$ is met for the spin triad (see above). Almost no transformations of the spectra are observed in the temperature interval $70 < T \leq 110$ K (see Fig. 8); this means that the spin transition was completed at temperatures below 110 K and allows one to estimate $|J| > 2kT \approx 150$ cm^{-1} at $T < 110$ K. The X- and Q-band EPR spectra obtained at $T = 70$ and 110 K are correctly approximated using the *g*-tensors $\boldsymbol{g}^{Cu} = [2.054; 2.084; 2.320]$ ($T = 70$ K) and $\boldsymbol{g}^{Cu} = [2.048; 2.078; 2.314]$ ($T = 110$ K). Close values of the corresponding components suggest that at $T < 70$ K one has $\boldsymbol{g}_{eff} \approx \boldsymbol{g}^{A} \approx [1.993; 1.983; 1.905]$. Most likely, a slight decrease in μ_{eff} at $50 < T < 110$ K is mainly due to antiferromagnetic intercluster interactions between the spin triads and the spins of the copper ions in the CuN_2O_4 sites. At temperatures above the spin transition temperature ($T > 150$ K), the Q-band EPR spectra exhibit a single broadened EPR line due to electron spin exchange (see above). This line is almost not shifted between 160 and 240 K, which means that the limit $|J|/kT \ll 1$ is reached. At 160 K, the effective *g*-factor of this line is $g_{eff} \approx 2.03$, being in accordance with the condition $|J|/kT < 1$ (see Fig. 7). Thus, the temperature dependence of the EPR spectra of $Cu(hfac)_2L^{Bu^n} \cdot 0.5C_7H_{16}$ reflects an abrupt spin transition occurring in three-spin exchange clusters $>N—^{\bullet}O—Cu^{2+}—O^{\bullet}—N<$ on going from the case $|J|/kT < 1$ to the case $|J|/kT > 1$.

$Cu(hfac)_2L^{Bu^n} \cdot 0.5C_7H_8$ provides an example of a compound characterized by a much smaller amplitude of the spin transition (see Fig. 2, *c*). The dependence $\mu_{eff}(T)$ shows quite a smooth transition in the temperature interval from nearly 140 to 70 K with the amplitude $\Delta\mu_{eff} \approx 0.32$. At 70 K, one has $\mu_{eff} \approx 2.15$ and, therefore, $|J|/kT \approx 0.6$; as a consequence, one shouled expect $g_{eff} \approx 2.03 > 2$ (see Fig. 7). Indeed, experimental EPR spectra are in excellent agreement with these assumptions (Fig. 9). Experiments in the X-band do not allow one to observe noticeable changes in the EPR spectra before and after the phase transition. Attempts to resolve the lines of the spin triad and magnetically isolated copper ion in the Q- and W-bands also failed. However, the W-band EPR spectra clearly demonstrate changes in the lineshape in the region $g \approx 2$ (see Fig. 9, *b*), which can be explained by the shift toward the high magnetic field (smaller values of the *g*-factor) of the still poorly resolved EPR line of the spin triad. The shape of the spin triad line in the W-band at 50 K also does not exclude the presence of more than one type of spin triads characterized by different exchange constants after the spin transition; however, the lack of intense signals with $g < 2$ is undoubtful. This suggests that the decrease in g_{eff} of the spin triad during the spin transition does occur as expected, but the amplitude Δg_{eff} is too small to be detected in the W-band. In other words, one deals with a weak exchange interaction within the triad (or effective averag-

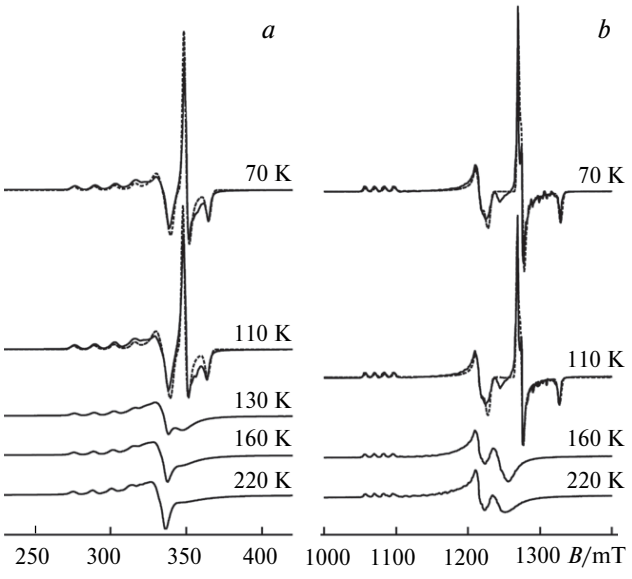

Fig. 8. Temperature dependences of EPR spectra of polycrystalline $Cu(hfac)_2L^{Bu^n} \cdot 0.5C_7H_{16}$ at 9 (*a*) and 34 GHz (*b*). Dashed lines denote simulated EPR spectra.

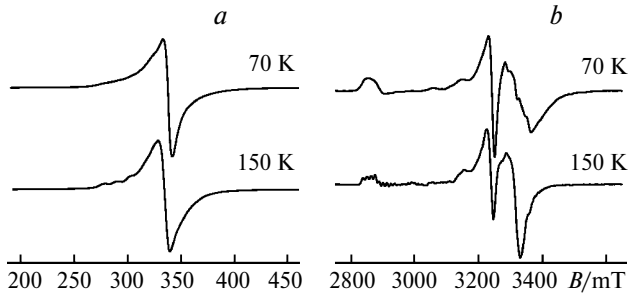

Fig. 9. Temperature dependences of EPR spectra of polycrystalline $Cu(hfac)_2L^{Bu^n} \cdot 0.5C_7H_8$ at 9 (*a*) and 94 GHz (*b*).

ing of exchange interaction between several types of triads); the exchange constant (or its averaged value) can be estimated from the condition $|J| < kT \approx 35$ cm^{-1}.

Using numerous examples, we have shown that the model developed for theoretical description allows one to establish correlations between the manifestations of spin transitions in EPR spectroscopy and in the magnetic susceptibility technique and to make simple estimates of the constants of the exchange interaction within spin triads. In the vast majority of compounds from the family of "breathing crystals", the magnetic moment decreases as temperature decreases; this can occur abruptly or smoothly, or proceed in a stepwise fashion. Compound Cu(hfac)$_2$L^{Et} is of particular interest because it demonstrates a different type of the dependence $\mu_{eff}(T)$ (see Fig. 2, *d*). As temperature decreases in the interval ~300—226 K, the magnetic moment decreases, thus demonstrating a rather strong antiferromagnetic exchange interaction within the spin triad. Nevertheless, an abrupt spin transition at $T_c \approx 226$ K ($\Delta T_c \approx 5$ K) causes μ_{eff} to increase by a value of nearly 0.15. This can be explained by rapid weakening of the antiferromagnetic exchange interaction or even by the change in the sign of the parameter J after the spin transition. In any case, this type of spin transition should lead to an "inverse" shift of (*i.e.*, an increase in) g_{eff} in contrast to all cases discussed above. It is just the trend shown by comparison of the W-band EPR spectra at 240 and 200 K (Fig. 10). The EPR lines of the isolated copper ion and the spin triad are unresolved; however, the shift of the high-field components of the spectrum toward the low-field region at 200 K is clearly seen. Thus, the example of Cu(hfac)$_2$L^{Et} demonstrates that the approach we have developed can be used for the detection and description of "inverse" spin transitions in heterospin exchange clusters where the ratio $|J|/kT$ decreases as temperature decreases.

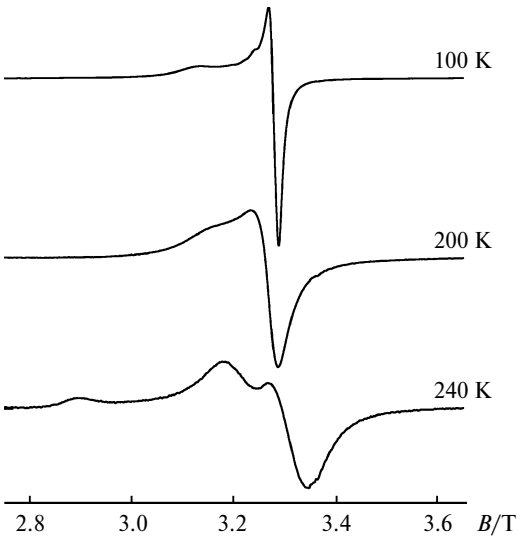

Fig. 10. Temperature dependence of W-band EPR spectra of polycrystalline Cu(hfac)$_2$L^{Et} at 94 GHz.

Temperature dependence of the exchange interaction constant

In the vast majority of exchange-coupled clusters used in studies of molecular magnetism, the exchange interaction constant (J) is temperature-independent. Even if the variations of the exchange constant could be observed, they were relatively small (*e.g.*, at most 1 cm^{-1}) (see Ref. 52). The polymer-chain complexes Cu(hfac)$_2$L^R we have studied belong to a specific class of compounds, which is characterized by significant variations of the geometry of exchange clusters with temperature and, as a consequence, by considerable changes in both intracluster and intercluster exchange interactions.

As mentioned above, in the presence of fast electron spin exchange the temperature dependence of the effective g-factor of the spin triad $g_{eff}(T)$ can be written using the g-factors of the nitroxide radical and copper(II) ion and Eq. (5). Thus, the position (effective g-factor) of an EPR line depends on the relative populations of multiplets of the strongly coupled triad and is therefore directly related to the exchange constant. The experimental dependence $g_{eff}(T)$ can be obtained by two approaches using a polycrystalline sample or a single crystal. Both methods have their advantages and drawbacks and can generally be combined to achieve the optimum result.

Difficulties in the experiments with polycrystalline samples include (1) overlap of the EPR lines of the spin triad and the magnetically isolated ion at high temperatures (this can be avoided using high-frequency EPR) and, as a consequence, (2) a decrease in the intensity of the EPR line of the spin triad because of the strong broadening in the high-field experiments. As a result, recording a high-quality EPR spectrum of the spin triad from the polycrystalline sample in the desired temperature range is difficult. In addition, since the EPR spectrum of the triad is anisotropic at $|J| >> kT$, the effective g-factor to be used in expression (5) should be calculated from the measured spectrum. Nevertheless, in the absence of single crystals this technique can be used to obtain the dependence $g_{eff}(T)$ and to calculate the desired function $J(T)$.

When using single crystals, the experimental dependence $g_{eff}(T)$ for the spin triad can be obtained much easier. The signals of the spin triad and the isolated ion can be separated with certainty at particular orientations of the single crystal even in the X-band EPR. It is noteworthy that the spectrum of the triad always represents an intense singlet line and usually it is not a problem to record high-quality EPR spectra. However, in the case of single crystals one should take into account the fact that the structural transition involves a change in the direcion of the long axis of the CuO_6 octahedron and, thus, the directions

of the axes of the *g*-tensor of the ion from the spin triad. The $g_{eff}(T)$ dependence thus obtained cannot be approximated by expression (5) because one should also take into account the temperature dependence of the *g*-factor of the copper(II) ion. At many orientations of the crystal, the g^{Cu} value varies only slightly and the function $g^{Cu}(T)$ can quite correctly be approximated using the g^{Cu} values at the high and low temperatures and the X-ray data. Nevertheless, the appearance of additional variables in the method for calculations of the dependence $J(T)$ makes the results obtained less reliable. In this connection, we do not stop efforts aimed at optimizing the accuracy of methods for the determination of the dependence $J(T)$.

A strong temperature dependence of the exchange interaction within the spin triads in "breathing crystals" is of great importance. This was already discussed in the previous Sections, but can most clearly be demonstrated by $J(T)$ measurements for the compounds exhibiting gradual changes in bond lengths and magnetic parameters as an example. In particular, the complex $Cu(hfac)_2L^{Bu^n} \cdot 0.5C_8H_{18}$ undergoes a smooth spin transition in the temperature range ~70 < *T* < 180 K. Figures 11 *a*, *b* show the observed temperature dependences of the position of the EPR line of the spin triad. From these data, the temperature dependence of the effective *g*-factor can be extracted with ease. The temperature dependence of the intracluster exchange constant $J(T)$ (see Fig. 11, *c*) was obtained by simulating the experimental dependence $g_{eff}(T)$ using expression (5). The *g*-factor of the Cu^{2+} ion in the spin triad was determined from the low-temperature EPR spectrum (60 K) while the value $g = 2.007$ determined previously was used for the *g*-factor of the nitroxide radical. The width of the $J(T)$ distribution obtained in the intermediate region is due to experimental error in the determination of the *g*-factor (±0.0005), which was taken into account in the simulation of the dependence $g_{eff}(T)$. At low temperatures, the dependence $g_{eff}(T)$ reaches a plateau, which corresponds to a range of possible values of the exchange interaction constant at which the condition (5) is met.

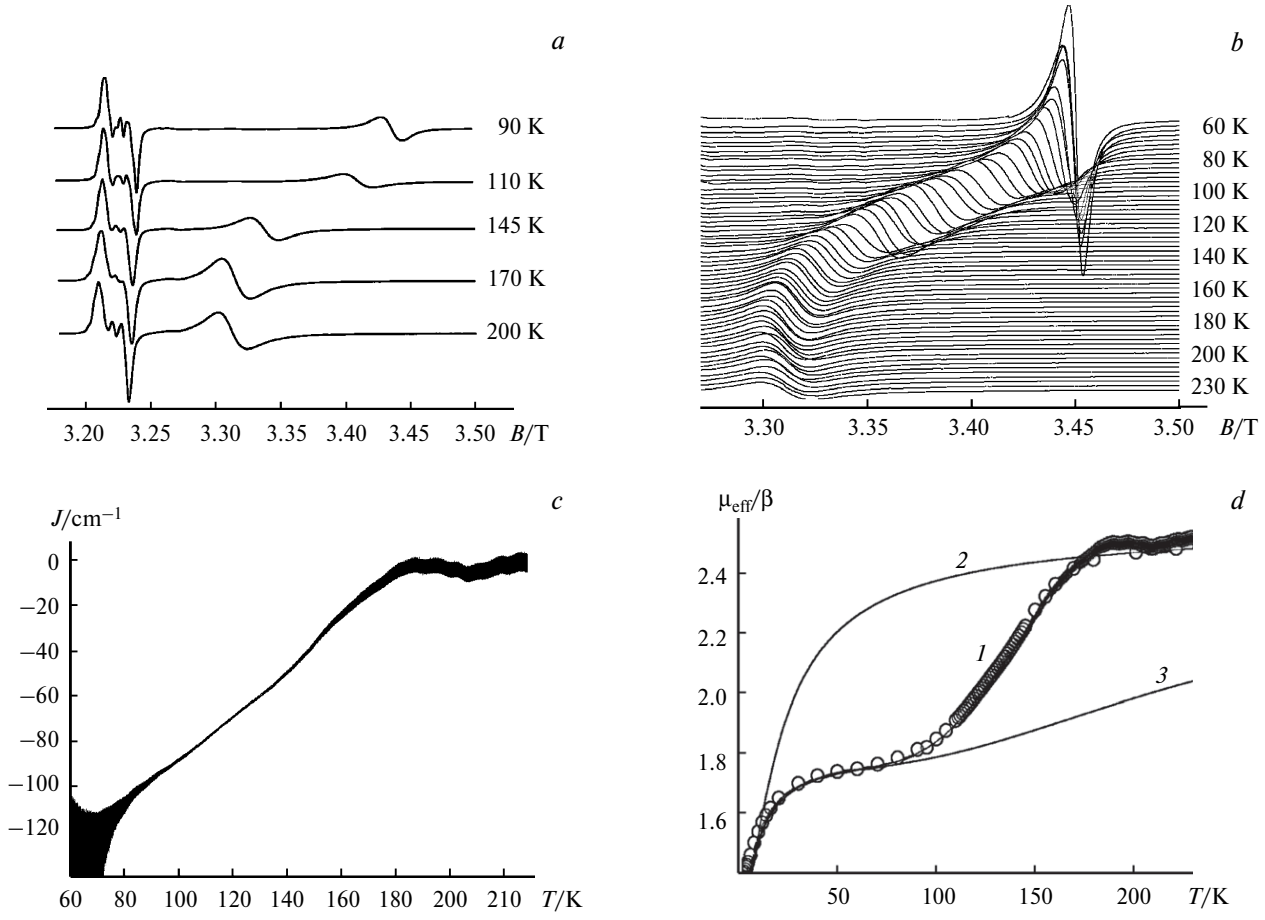

Fig. 11. Temperature dependences of W-band (94 GHz) EPR spectra of a $Cu(hfac)_2L^{Bu^n} \cdot 0.5C_8H_{18}$ single crystal (*a*). High-resolution temperature dependence of a line of the spin triad (*b*). Temperature dependence of the exchange constant (*c*). Experimental dependence of the magnetic susceptibility $\mu_{eff}(T)$ (open circles) and the theoretical dependences $\mu_{eff}(T)$ calculated using the $J(T)$ function (*1*) and the constant exchange interaction values $J = -10$ cm^{-1} (*2*) and -120 cm^{-1} (*3*) (*d*).

The dependence $J(T)$ can be used to calculate the effective magnetic moment $\mu_{eff}(T)$ of $Cu(hfac)_2L^{Bu^n} \cdot C_8H_{18}$ in order to compare it with the experimental value (see Fig. 11, *d*). In the simulation of $\mu_{eff}(T)$, the intercluster exchange interaction was taken into account as described elsewhere.[53,54] Agreement between the simulated and experimental dependences $\mu_{eff}(T)$ in the whole temperature range is an independent evidence of the correctness of the $J(T)$ dependence. It should be noted that simulation of the experimental temperature dependences of the effective *g*-factor and magnetic moment ($g_{eff}(T)$ and $\mu_{eff}(T)$, respectively) using a constant exchange interaction value is impossible, as is clearly demonstrated in Fig. 11, *d* for the $\mu_{eff}(T)$ dependence taking two values of the exchange constant J ($J = -10$ cm^{-1} and $J = -120$ cm^{-1}) as examples.

Light-induced spin transitions and excited spin state trapping

"Breathing crystals" can undergo reversible thermally induced spin transitions, which are very similar to classical spin crossover. This property is key to potential applications of such systems in spintronics.[55,56] However, optical manipulation of the magnetization is undoubtedly much more convenient from the standpoint of future practical applications. Optically induced switching of the spin state is well known for many iron complexes that undergo a classical spin crossover.[57–64] Moreover, light-induced excited spin state trapping (LIESST) in these compounds was also discovered and studied. The phenomenon is that the excited spin state induced by the laser irradiation is metastable on the time scale from a few hours to a few days at sufficiently low temperatures (typically, at $T < 50$ K). In connection to the fact that spin transitions in "breathing crystals" are highly similar to the classical spin crossover, there were grounds to believe that light-induced switching of the spin state is possible for them.

Our first experiments involved photoexcitation of compounds from the family of "breathing crystals" $Cu(hfac)_2L^R$ and detection of the excited state by EPR spectroscopy. Prior to our expeiments, LIESST was observed in many iron complexes that undergo spin crossover. In all cases including exchange-coupled multinuclear complexes, it is spin crossover in the iron complexes that is responsible for the manifestation of LIESST. We have reported the first example of LIESST in a fundamentally different type of systems, *viz.*, exchange-coupled clusters comprising copper and two nitronyl-nitroxide radicals.[36] These systems contain no metals exhibiting spin crossover and conversion of the spin state occurs in the exchange-coupled spin triad. In our experiments, changes in the spin state were detected from the Q-band EPR spectra (Fig. 12) using different detection techniques (c.w. detection and time-resolved EPR). Both of them are suitable for the detection of LIESST in "breathing crystals" on the corresponding time scales. Time-resolved EPR spectroscopy allows one to detect the formation and the primary structural and electronic relaxation of the excited state on the microsecond time scale, while c.w. EPR spectroscopy is approapriate for investigations of slow relaxation of the "trapped' spin state. When exposed to monochromatic light ($\lambda = 900$ nm) at 7 K, the degree of conversion from the strongly coupled to the weakly coupled spin state was as high as 80%. After photoexcitation, the spin triad relaxes back to the strongly coupled state on the time scale of the order of a few hours (see Fig. 12, *a*, *c*). However, raising the temperature of the sample to 20 K over a period of a few minutes followed by cooling to 7 K causes the system to return to the initial state (see Fig. 12, *a*). These features are similar to many observations of LIESST in iron complexes. Note that practical implementation of the "classical" experimental design for the detection of LIESST in the "breathing crystals" under study upon irradiation of the sample placed inside the SQUID-magnetometer is a very complicated task. These heterospin crystals are deeply colored and characterized by numerous intense absorption bands in the UV, visible, and IR regions. Therefore, light only slightly penetrates into the crystal, being absorbed in the near-surface layer, which causes its heating. We have developed a method of dilution of the sample with a transparent substrate to detect LIESST in the probe of an EPR spectrometer (see Ref. 36). We also proposed the mechanism of formation of LIESST in "breathing crystals", which will be studied in detail in the future. It should be noted that we also have discovered LIESST in some other compounds of the family $Cu(hfac)_2L^R$. This suggests that LIESST is common to "breathing crystals", which makes them promising for the use in light-controlled molecular devices and in data storage and processing devices.

Studies of exchange interactions in two-spin clusters

In the previous Sections, we have considered the results of studies on the "breathing crystals" $Cu(hfac)_2L^R$ with the "head-to-head" chain motif. However, as mentioned above, the family $Cu(hfac)_2L^R$ also includes complexes with the "head-to-tail" motif; their polymeric chains include two-spin copper(II)—nitroxide clusters. One of a few representatives of this type of compounds is the complex $Cu(hfac)_2L^{Me}$ whose polymer-chain structure is shown in Fig. 1, *b*. In spite of apparent regular character of the chain, lowering the temperature to 230 K is accompanied by irreversible doubling of the unit cell and formation of alternating nonidentical two-spin clusters.

Structural rearrangements in the polymeric chain of $Cu(hfac)_2L^{Me}$ mainly occur on cooling to the structural phase transition temperature ($T_c^{\downarrow} = 141$ K) and lead to an abrupt decrease in μ_{eff} by a factor of $\sqrt{2}$, which indicates "disappearance" of 50% of spins with $S = 1/2$ in the sam-

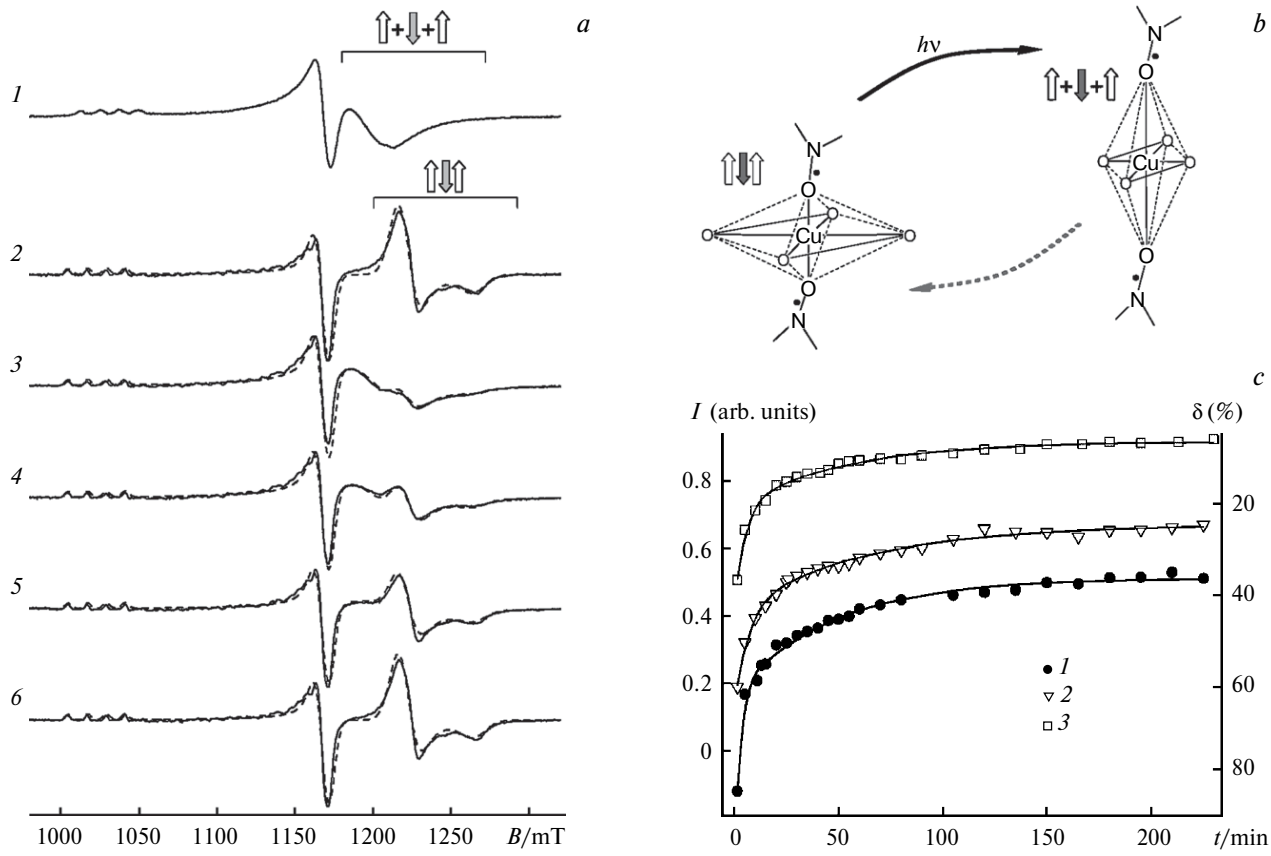

Fig. 12. Q-band EPR studies of light-induced switching of the spin state and LIESST in complex $Cu(hfac)_2L^{Pr^n}$. EPR spectra at 180 K (*1*); EPR spectra at 7 K recorded before (*2*) and immediately after exposure to light (λ = 900 nm) over a period of 90 s (*3*), those obtained 5 (*4*) and 180 min (*5*) after irradiation, and after subsequent heating to 20 K followed by cooling to 7 K (*6*). Simulated spectra are shown by dashed lines (*a*). A schematic presentation of light-induced conversion (*b*). The intensity (*I*) of the EPR signal of the spin triad (B = 1216 mT) and the degree of conversion (δ) plotted *vs.* time at 7 K (*1*), 10 K (*2*), and 13 K (*3*) (*c*).

ple (Fig. 13). As a result, in 50% of coordination sites the inter-spin distances Cu—O_L are shortened and, as a consequence, antiferromagnetic exchange interaction is abruptly increased. The other 50% of exchange clusters are characterized by insignificant variations of their geometries and weak ferromagnetic exchange interaction still dominates.

At temperatures above 141 K, the EPR spectrum of polycrystalline $Cu(hfac)_2L^{Me}$ represents a broad singlet line ($g \approx 2.1$, $\Gamma_{pp} \approx 30$ mT) with unresolved structure. Most likely, this is due to the strong exchange interaction between neighboring clusters (see Fig. 13). A narrow line at $g \approx 2.007$ also observed in the spectrum represents the signal of defects, namely, nitroxide radicals formed in the course of preparation of the polycrystalline sample. After phase transition (at $T < T_c^{\downarrow}$), the EPR spectrum changes significantly and exhibits a number of characteristic features typical of the triplet states, including the "forbidden" double-quantum half-field transitions (see Fig. 13). The triplet state observed can unambiguously be assigned to the two-spin copper—nitroxide clusters linked through weak ferromagnetic interaction (the "second" type of clusters). The EPR spectra of the single crystal recorded at different

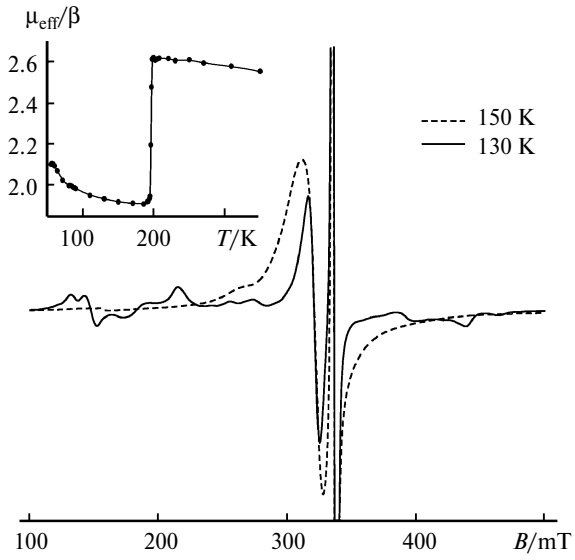

Fig. 13. EPR spectra of polycrystalline $Cu(hfac)_2L^{Me}$ at temperatures above (150 K) and below (130 K) the transition temperature. Inset: temperature dependence of the effective magnetic moment μ_{eff}.

orientations of the sample relative to the magnetic field show the same thermally induced feature as the spectra of the polycrystalline sample (Fig. 14). At temperatures above the transition temperature, there is also a singlet line whose width is strongly dependent on the orientation of the single crystal (see Fig. 14, *a*). Below the structural phase transition temperature ($T < T_c^{\downarrow}$), the EPR spectra of the single-crystalline sample correspond to the spectra of a triplet state with a typical orientation dependence of the splitting, which is due to dipole—dipole interaction (see Fig. 14, *b*).

Since the integrated intensity of the EPR spectrum is halved after the phase transition, the signals observed at $T < T_c^{\downarrow}$ undoubtfully correspond to the remaining 50% of two-spin clusters in which no spin pairing occurred. The first 50% of clusters became diamagnetic due to strong antiferromagnetic exchange and thus are not observed in the EPR spectrum. For the same reason, the exchange channels between the remaining paramagnetic clusters are now less efficient, *i.e.*, we deal with efficient diamagnetic dilution of the sample, which made it possible to observe a resolved structure of the EPR lines at $T < T_c^{\downarrow}$.

The experimental EPR spectrum of a single crystal of $Cu(hfac)_2L^{Me}$ (Fig. 14, *c*) corresponds to an angle of rotation of 40° at 130 K (see Fig. 14, *b*). The angular dependence of the spectra is due to anisotropic dipole—dipole interaction and the observed splitting of the components of the doublet into triplets can be attributed to weak isotropic exchange interaction between two-spin clusters. Let the spin Hamiltonian of the system have the form:

$$\hat{H} = \beta \boldsymbol{B} \boldsymbol{g}_{cl} \boldsymbol{S}_1 + D(S^2_{1z} - \boldsymbol{S}^2_1) + E(S^2_{1x} - S^2_{1y}) + \beta \boldsymbol{B} \boldsymbol{g}_{cl} \boldsymbol{S}_2 + \\ + D(S^2_{2z} - \boldsymbol{S}^2_2) + E(S^2_{2x} - S^2_{2y}) - 2J_{cl-cl} \boldsymbol{S}_1 \boldsymbol{S}_2, \quad (7)$$

where $\boldsymbol{g}_{cl}$ is the *g*-tensor of the copper(II)—nitroxide cluster; $\boldsymbol{B} = [0,0,B]$ is the magnetic field parallel to the *Z* axis; *D* and *E* are zero-field splitting parameters; and J_{cl-cl} is the isotropic exchange interaction between two clusters with effective spins $S = 1$.

Using the values $g_{cl} = [2.04\ 2.07.\ 2.14]$, $D = \pm 120$ mT, $E = \pm 32$ mT, $J_{cl-cl} = 25$ mT, one can attain reasonable qualitative agreement in calculations of the whole angular dependence of the EPR spectra. However, the model including two interacting clusters and described by the Hamiltonian (7) requires substantiation, because each exchange cluster Cu—O_L has two neighbors (not one!) within a particular chain; in turn, these two neighbors are bound to their own neighbors. In this connection, one should understand which clusters are involved in the exchange interaction observed. According to X-ray data, at $T < T_c^{\downarrow}$ the distance between the neighboring paramagnetic clusters within the same polymeric chain (Cu—Cu, 14.189 Å) is too long to explain the exchange interaction observed. The shortest Cu—Cu distance between the paramagnetic clusters in different chains is also rather long (8.743 Å).

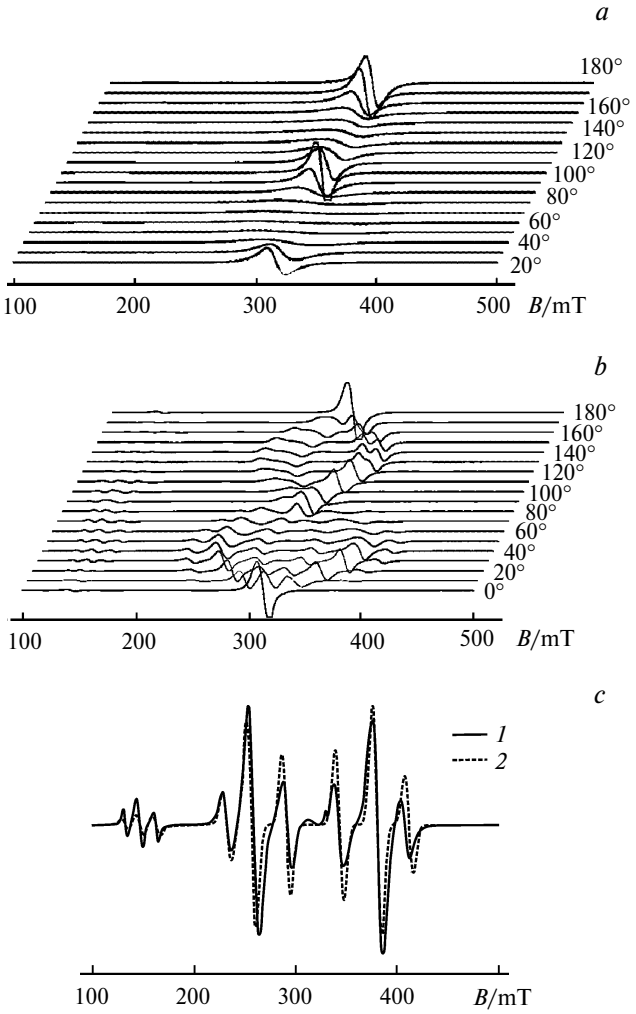

Fig. 14. EPR spectra of $Cu(hfac)_2L^{Me}$ single crystal recorded at different orientations of the sample relative to the magnetic field at temperatures above (150 K) (*a*) and below (130 K) (*b*) the transition temperature; the experimental (*1*) and simulated (*2*) EPR spectra corresponding to an angle of 40° at 130 K (*c*).

However, the spin density of the unpaired electron of the ligand is not localized on the coordinated oxygen atom; rather, it is symmetrically distributed over the imidazolidine ring and has maxima on both oxygen atoms. At $T < T_c^{\downarrow}$, in the crystal structure of $Cu(hfac)_2L^{Me}$ all exchange clusters with the effective spin $S = 1$ can be divided into pairs in which the distance between uncoordinated oxygen atoms is of the order of 3.9 Å. This distance is only two times longer than the characteristic Cu—O bond length and can therefore serve as a channel of the exchange interaction of the corresponding clusters. It is noteworthy that these clusters belong to the neighboring chains rather than the same polymeric chain.

Thus, effective diamagnetic dilution of the sample as a result of structural and spin transitions offers prospects for EPR studies of weak intercluster interactions in

$Cu(hfac)_2L^{Me}$. In addition, the interaction between clusters belonging to neighboring chains demonstrates the potential importance of studies of these exchange channels in other polymer-chain complexes $Cu(hfac)_2L^R$.

Conclusion

Our studies reviewed here revealed a high informativity of EPR spectroscopy in different frequency bands in the research on "breathing crystals" $Cu(hfac)_2L^R$. They are the magnetically concentrated crystals containing paramagnetic two- and three-spin clusters of Cu^{2+} with nitroxide radicals characterized by typical exchange interaction constants of the order of tens to hundreds of reciprocal centimeters. Often, such systems exhibit strongly broadened or exchange-narrowed unresolved EPR lines and EPR spectroscopy thus becomes little informative. Contrary to this, we have shown that one can obtain key information on exchange interactions and measure the temperature dependence $J(T)$ in "breathing crystals" $Cu(hfac)_2L^R$ despite the fact that the energy of exchange interaction is a few orders of magnitude higher than that of a microwave field quantum. This becomes possible owing to the fact that the typical values of the exchange interaction constants for compounds $Cu(hfac)_2L^R$ become comparable with the thermal energy kT in the temperature range 4—300 K. As a consequence, in this temperature range the populations of different multiplets in the spin triads and the EPR spectra are significantly changed; a detailed analysis of these parameters makes it possible to obtain the necessary information. Using this feature of the compounds under examination, we developed a number of methods of qualitative and quantitative analysis of exchange interactions within the nitroxide—copper—nitroxide spin triads. In studies of two-spin copper—nitroxide clusters, information on weak intercluster exchange interaction was obtained by EPR spectroscopy. In addition, having understood specific features of EPR spectroscopy of "breathing crystals" and the distinctive features of the signals of the strongly and weakly coupled spin triads, we carried out experimental studies on the effect of light on the spin transitions in "breathing crystals" and for the first time demonstrated a light-induced conversion and excited spin state trapping at low temperatures.

Summing up, the review presents the state of the art in EPR studies of themally induced and light-induced spin transitions within exchange clusters in "breathing crystals". A number of issues, first of all those concerned with investigations of intercluster exchange interactions, the mechanism and specific features of light-induced spin conversion and relaxation of the excited state are still to be solved. Further investigations will gain a better insight into the new class of effects appeared upon nonclassical spin transitions and are of practical interest from the standpoint of research on the potential of "breathing crystals" for the design of functional magneto-active nanomaterials.

This work was financially supported by the Russian Foundation for Basic Research (Project Nos 08-03-00326 and 09-03-00091), the Council on Grants at the President of the Russian Federation (Program of State Support of Young Candidates of Science MK-60.2008.3 and MK-4268.2010.3), the Presidium of the Russian Academy of Science (Program No. 18.13), Alexander von Humboldt Foundation (AvH, M. F.), the Federal Agency for Science and Innovations (under State Contract No. 02.513.12.3098), and the Federal Agency for Education (NK 24P/1).

References

1. O. Kahn, *Molecular Magnetism*, VCH, New York, 1993, 380.
2. *Molecular Magnetism: From Molecular Assemblies to the Devices,* Eds E. Coronado, P. Delhaès, D. Gatteschi, J. S. Miller, Kluwer Academic Publisher, Dordrecht, 1996, **321**.
3. *Molecular Magnetism*, Eds K. Itoh, M. Kinoshita, Kodansha Ltd. and Gordon and Breach Science Publisher, Amsterdam—London, 2000.
4. *Magnetism: Molecules to Materials I. Models and Experiments*, Eds J. S. Miller, M. Drillon, Wiley-VCH, Weinheim—New York, 2001, 437.
5. *Molecular Magnets: Recent Highlights*, Eds W. Linert, M. Verdaguer, Springer-Verlag, Wien—New York, 2003.
6. A. Caneschi, D. Gatteschi, P. Rey, *Prog. Inorg. Chem.*, 1991, **39**, 331.
7. V. I. Ovcharenko, R. Z. Sagdeev, *Usp. Khim.*, 1999, **68**, 381 [*Russ. Chem. Rev.* (*Engl. Transl.*), 1996, **68**, 345].
8. S. S. Eaton, G. R. Eaton, *Coord. Chem. Rev.*, 1978, **26**, 207.
9. S. S. Eaton, G. R. Eaton, *Coord. Chem. Rev.,* 1988, **83**, 29.
10. S. V. Larionov, *Imidazoline Nitroxides. Synthesis, Properties and Applications*, Ed. L. B. Volodarsky, CRC Press, Boca Raton, 1988, **2**, 81.
11. L. B. Volodarsky, V. A. Reznikov, V. I. Ovcharenko, *Synthetic Chemistry of Stable Nitroxides,* CRC Press, Boca Raton, 1994, 225.
12. G. A. Abakumov, *Zh. Vsesoyuz. Khim. O-va im. D. I. Mendeleeva,* 1979, **24**, 156 [*Mendeleev Chem. J.* (*Engl. Transl.*), 1979, **24**].
13. H. Iwamura, K. Inoue, T. Hayamizu, *Pure Appl. Chem.*, 1996, **68**, 243.
14. D. Luneau, P. Rey, *Coord. Chem. Rev.,* 2005, **249**, 2591.
15. D. Luneau, A. Borta, Y. Chumakov, J.-F. Jacquot, E. Jeanneau, C. Lescop, P. Rey, *Inorg. Chim. Acta*, 2008, **361**, 3669.
16. A. Caneschi, D. Gatteschi, R. Sessoli, P. Rey, *Acc. Chem. Res.*, 1989, **22**, 392.
17. *Magnetism: Molecules to Materials II. Molecule-Based Materials*, Eds J. S. Miller, M. Drillon, Wiley-VCH, Weinheim, 2001, 489.
18. H. Oshio, T. Ito, *Coord. Chem. Rev.,* 2000, **198**, 329.
19. L. Ouahab, *Coord. Chem. Rev.*, 1998, **178—180**, 1501.
20. O. Sato, J. Tao, Y-Z. Zhang, *Angew. Chem.*, *Int. Ed.*, 2007, **46**, 2152.
21. K. E. Vostrikova, *Coord. Chem. Rev.,* 2008, **252**, 1409.

22. A. L. Buchachenko, *Usp. Khim.*, 1990, **59**, 529 [*Russ. Chem. Rev.* (*Engl. Transl.*), 1990, **59**, 307].
23. E. Yu. Fursova, V. I. Ovcharenko, *Zh. Vseros. Khim. O-va im. D. I. Mendeleeva*, 2009, **53**, 23 [*Mendeleev Chem. J.* (*Engl. Transl.*), 2009, **53**].
24. A. Bencini, D. Gatteschi, *Electron Paramagnetic Resonance of Exchange-Coupled Systems*, Springer-Verlag, Berlin—Heidelberg, 1990, 287.
25. D. Gatteschi, A. L. Barra, A. Caneschi, A. Cornia, R. Sessoli, L. Sorace, *Coord. Chem. Rev.*, 2006, **250**, 1514.
26. E. J. L. McInnes, *Sruct. Bond.*, 2006, **122**, 69.
27. R. Z. Sagdeev, Yu. N. Molin, R. A. Sadikov, L. B. Volodarsky, G. A. Kutikova, *J. Magn. Reson.*, 1973, **9**, 13.
28. S. Piligkos, E. Bill, D. Collison, E. J. L. McInnes, G. A. Timco, H. Weihe, R. E. P. Winpenny, F. Neese, *J. Am. Chem. Soc.*, 2007, **129**, 760.
29. J. Yoon, L. M. Mirica, T. D. P. Stack, E. I. Solomon, *J. Am. Chem. Soc.*, 2004, **126**, 12586.
30. R. Ziessel, C. Stroh, H. Heise, F. H. Kohler, P. Turek, N. Claiser, M. Souhassou, C. Lecomte, *J. Am. Chem. Soc.*, 2004, **126**, 12604.
31. K. Maekawa, D. Shiomi, T. Ise, K. Sato, T. Takui, *J. Phys. Chem. B*, 2005, **109**, 3303.
32. M. Fedin, S. Veber, I. Gromov, V. Ovcharenko, R. Sagdeev, A. Schweiger, E. Bagryanskaya, *J. Phys. Chem. A*, 2006, **110**, 2315.
33. M. Fedin, S. Veber, I. Gromov, V. Ovcharenko, R. Sagdeev, E. Bagryanskaya, *J. Phys. Chem. A*, 2007, **111**, 4449.
34. M. Fedin, S. Veber, I. Gromov, K. Maryunina, S. Fokin, G. Romanenko, R. Sagdeev, V. Ovcharenko, E. Bagryanskaya, *Inorg. Chem.*, 2007, **46**, 11405.
35. S. L. Veber, M. V. Fedin, A. I. Potapov, K. Yu. Maryunina, G. V. Romanenko, R. Z. Sagdeev, V. I. Ovcharenko, D. Goldfarb, E. G. Bagryanskaya, *J. Am. Chem. Soc.*, 2008, **130**, 2444.
36. M. Fedin, V. Ovcharenko, R. Sagdeev, E. Reijerse, W. Lubitz, E. Bagryanskaya, *Angew. Chem., Int. Ed.*, 2008, **47**, 6897.
37. S. L. Veber, M. V. Fedin, K. Yu. Maryunina, G. V. Romanenko, R. Z. Sagdeev, E. G. Bagryanskaya, V. I. Ovcharenko, *Inorg. Chim. Acta*, 2008, **361**, 4148.
38. M. V. Fedin, S. L. Veber, G. V. Romanenko, V. I. Ovcharenko, R. Z. Sagdeev, G. Klihm, E. Reijerse, W. Lubitz, E. G. Bagryanskaya, *Phys. Chem. Chem. Phys.*, 2009, **11**, 6654.
39. V. I. Ovcharenko, S. V. Fokin, G. V. Romanenko, Yu. G. Shvedenkov, V. N. Ikorskii, E. V. Tret´yakov, S. F. Vasilevskii, *Zh. Struktur. Khim.*, 2002, **43**, 163 [*J. Struct. Chem.* (*Engl. Transl.),* 2002, **43**].
40. P. Rey, V. I. Ovcharenko, in *Magnetism: Molecules to Materials IV*, Eds J. S. Miller, M. Drillon, Wiley-VCH, Weinheim—New York, 2003, p. 41.
41. V. I. Ovcharenko, S. V. Fokin, G. V. Romanenko, V. N. Ikorskii, E. V. Tretyakov, S. F. Vasilevskii, R. Z. Sagdeev, *Mol. Phys.*, 2002, **100**, 1107.
42. V. I. Ovcharenko, K. Yu. Maryunina, S. V. Fokin, E. V. Tret´yakov, G. V. Romanenko, V. N. Ikorskii, *Izv. Akad. Nauk. Ser. Khim.*, 2004, 2304 [*Russ. Chem. Bull., Int. Ed.*, 2004, **53**, 2406].
43. V. I. Ovcharenko, G. V. Romanenko, K. Yu. Maryunina, A. S. Bogomyakov, E. V. Gorelik, *Inorg. Chem.*, 2008, **47**, 9537.
44. Yu. V. Yablokov, V. K. Voronkova, L. V. Mosina, *Paramagnitnyi rezonans obmennykh klasterov* [*Paramagnetic Resonance in Exchange Clusters*], Nauka, Moscow, 1988, 181 (in Russian).
45. L. Banci, A. Bencini, D. Gatteschi, *Inorg. Chem.*, 1983, **22**, 2681.
46. L. Banci, A. Bencini, A. Dei, D. Gatteschi, *Inorg. Chem.*, 1983, **22**, 4018.
47. C. Benelli, D. Gatteschi, C. Zanchini, J. M. Latour, P. Rey, *Inorg. Chem.*, 1986, **25**, 4242.
48. E. G. Boguslavskii, A. A. Shklyaev, V. F. Yudanov, V. I. Ovcharenko, S. V. Larionov, *Izv. Akad. Nauk SSSR. Ser. Khim.*, 1984, 1517 [*Bull. Acad. Sci. USSR, Div. Chem. Sci.* (*Engl. Transl.*), 1984, **33**, 1394].
49. V. B. Stryukov, D. N. Fedotin, A. V. Zvarykina, *Zh. Eksperim. Teor. Fiz.*, 1974, **19**, 687 [*J. Exp. Theor. Phys.* (*Engl. Transl.*), 1974, **19**].
50. S. Vancoillie, L. Rulíšek, F. Neese, K. Pierloot, *J. Phys. Chem. A*, 2009, **113**, 6149.
51. A. Carrington, A. McLachlan, *Introduction to Magnetic Resonance with Applications to Chemistry and Chemical Physics*, Harper and Row Publishers, New York, 1969, 204 p.
52. T. A. Kennedy, S. H. Choh, G. Seidel, *Phys. Rev. B*, 1970, **2**, 3645.
53. A. P. Ginsberg, M. E. Lines, *Inorg. Chem.*, 1972, **11**, 2289.
54. J. S. Smart, *Effective Field Theories of Magnetism*, W. B. Company, Philadelfia—London, 1966, 188.
55. V. A. Ivanov, T. G. Aminov, V. M. Novotortsev, V. T. Kalinnikov, *Izv. Akad. Nauk. Ser. Khim.*, 2004, 2255 [*Russ. Chem. Bull., Int. Ed.,* 2004, **53**, 2357].
56. C. Felser, G. H. Fecher, B. Balke, *Angew. Chem., Int. Ed.*, 2007, **46**, 668.
57. S. Decurtins, P. Gütlich, C. P. Kohler, H. Spiering, A. Hauser, *Chem. Phys. Lett.*, 1984, **105**, 1.
58. P. Gütlich, P. Poganiuch, *Angew. Chem., Int. Ed.*, 1991, **30**, 975.
59. P. Gütlich, A. Hauser, H. Spiering, *Angew. Chem., Int. Ed.*, 1994, **33**, 2024.
60. E. Breuning, M. Ruben, J.-M. Lehn, F. Renz, Y. Garcia, V. Ksenofontov, P. Gütlich, E. Wegelius, K. Rissanen, *Angew. Chem., Int. Ed.*, 2000, **39**, 2504.
61. F. Renz, H. Oshio, V. Ksenofontov, M. Waldeck, H. Spiering, P. Gütlich, *Angew. Chem., Int. Ed.*, 2000, **39**, 3699.
62. A. Hauser, *Topics in Current Chemistry*, Eds P. Gütlich, H. A. Goodwin, Springer-Verlag, Berlin—Heidelberg, 2004, **234**, P. 155.
63. S. Bonhommeau, G. Molnar, A. Galet, A. Zwick, J.-A. Real, J. J. McGarvey, A. Bousseksou, *Angew. Chem., Int. Ed.*, 2005, **44**, 4069;
64. O. Sato, J. Tao, Y.-Z. Zhang, *Angew. Chem., Int. Ed.*, 2007, **46**, 2152.

Received October 15, 2009